ELSEVIER

Journal of Materials Processing Technology 169 (2005) 83–88

Journal of Materials Processing Technology

www.elsevier.com/locate/jmatprotec

Simulation of thermal diffusivity of Al/NaCl powder compacts in producing Al foams by the sintering and dissolution process

D.X. Sun *, Y.Y. Zhao

Department of Engineering, University of Liverpool, L69 3GH Liverpool, UK

Received 26 February 2003; received in revised form 5 January 2005; accepted 15 February 2005

Abstract

In the sintering and dissolution process for manufacturing Al foams, effective sintering is crucial to achieve a strong bonding between the Al particles. In order to predict the time needed for the sintering temperature to be reached throughout an Al/NaCl compact, it is necessary to characterize its thermal diffusivity. This paper determines the thermal diffusivities of a series of Al/NaCl compacts by measuring their temperature profiles during heating and comparing them with computer simulations using Matlab. The thermal diffusivities are found to be in the region of 3×10^{-7} m^2/s and increase approximately linearly with increasing the weight fraction of Al in the compacts. They are much lower than those of the Al and NaCl, due to the existence of low-thermal-conductivity air in the compacts. The time needed for temperature homogenization is mainly determined by the geometry and size of the compact. The effect of Al weight fraction is less significant in comparison.

Keywords: Sintering; Al/NaCl powders; Thermal diffusivity; Simulation

1. Introduction

Al foams have recently attracted much attention from the materials community because of their lightweight and exceptional mechanical, thermal and acoustic properties [1–11]. Al foams have great potential for wide applications in the transport, construction and chemical industries. They can be used as sandwich panels, thermal insulators, heat exchangers, sound absorbers, filters and most importantly, energy absorbers. As Al foams can absorb large amount of energy under impact, their large-scale applications are likely to be in the automotive industry with an aim to improve the vehicle crashworthiness and thus passenger safety.

The sintering and dissolution process (SDP) is a novel method developed in the University of Liverpool [12–14]. In SDP, an Al or Al alloy powder is mixed with a NaCl powder at a pre-specified proportion and compressed into a compact under an appropriate pressure. Small amount of Mg powder is usually added in the powder mixture to improve the sintering process because Mg can absorb the air entrapped in the compact and reduce the oxide of Al, which prohibit effective sintering of Al. The compact is sintered at a temperature either slightly above or slightly below the melting point of the Al matrix for 2.5–50 h, depending on the composition and size of the compact. The sintered compact is placed in a hot water bath to dissolve the NaCl particles in the compact. An Al foam is obtained after the dissolution process. Among the currently available processing methods for producing Al foams [10–12], SDP is one of the most cost-effective routes. The main advantages of SDP are accurate control over the pore size and porosity, uniform distribution of pore size and porosity, a wide range of pore sizes from 0.1 to 3 mm, and net-shape capability.

The sintering stage is the most crucial part of SDP. To achieve a strong bonding between the Al particles, the Al/NaCl compact needs to be maintained at the elevated sintering temperature for a sufficient period of time. In the selection of heating time, both the homogenization time and

* Corresponding author. Present address: Department of Engineering, University of Hull, HU6 7RX Hull, UK. Tel.: +44 151 7944697; fax: +44 151 7944675.

E-mail addresses: d.sun@hull.ac.uk (D.X. Sun), y.y.zhao@liv.ac.uk (Y.Y. Zhao).

0924-0136/$ – see front matter © 2005 Elsevier B.V. All rights reserved.
doi:10.1016/j.jmatprotec.2005.02.263

Nomenclature

c	specific heat of Al/NaCl compact (J/(g K))
c_{air}	specific heat of air (J/(g K))
c_{Al}	specific heat of Al (J/(g K))
$c_{Al_2O_3}$	specific heat of Al_2O_3 (J/(g K))
c_{NaCl}	specific heat of NaCl (J/(g K))
f_{air}	volume faction of air in Al/NaCl compact
f_{Al}	volume faction of Al in Al/NaCl compact
$f_{Al_2O_3}$	volume faction of Al_2O_3 in Al/NaCl compact
f_{Nacl}	volume faction of NaCl in Al/NaCl compact
h	coefficient related to k_s, k and s
k	thermal conductivity of Al/NaCl (W/(m K))
k_{air}	thermal conductivity of air (W/(m K))
k_{Al}	thermal conductivity of Al (W/(m K))
$k_{Al_2O_3}$	thermal conductivity of Al_2O_3 (W/(m K))
k_{NaCl}	thermal conductivity of NaCl (W/(m K))
k_s	thermal conductivity of steel (W/(m K))
l	length of Al/NaCl compact (mm)
r	radial distance of Al/NaCl compact (mm)
R	radius of Al/NaCl compact (mm)
s	thickness of steel tube (mm)
t	time (s)
T	temperature of Al/NaCl compact (°C)
T_0	temperature of furnace (°C)
ΔT	temperature of change (°C)
w_{Al}	weight fraction of Al in Al/NaCl compact

Greek symbols

α	thermal diffusivity (m^2/s)
ρ	density of Al/NaCl compact (g/mm^3)
ρ_{air}	density of air (g/mm^3)
ρ_{Al}	density of Al (g/mm^3)
$\rho_{Al_2O_3}$	density of Al_2O_3 (g/mm^3)
ρ_{Nacl}	density of NaCl (g/mm^3)

the sintering time must be taken into account. The former is the time needed for the entire compact to reach the sintering temperature and the latter is the time needed for the formation of strong bonding in the Al matrix. While the surface of a compact placed into a furnace can reach the sintering temperature very quickly, it may take a long time before the central part of the compact also reaches the sintering temperature. The homogenization time is determined by the thermal diffusivity and the geometry of the compact. With a known thermal diffusivity, it is relatively easy to calculate the homogenization times for different sized compacts by solving the heat conduction equations. However, no thermal diffusivity data is currently available for Al/NaCl compacts. An Al/NaCl compact contains not only Al and NaCl but also some air and small amount of Al_2O_3. It is not clear to what extent the thermal diffusivity of a compact is affected by the Al–NaCl ratio and the unavoidable air and impurities.

This paper determines the thermal diffusivities of a series of Al/NaCl compacts by measuring their temperature profiles during heating and comparing them with the computer simulations using a general software package, Matlab, and discusses the effects of the composition and the density of the compacts on the thermal behaviour.

2. Measurements of temperature profiles

The precursor materials for the Al/NaCl compacts were a commercially pure gas atomized Al powder and a commercial NaCl powder with particle sizes in the ranges of 50–400 and 150–3000 μm, respectively. The NaCl powder was predried in an electrical furnace at 400 °C for at least 30 min. The NaCl powder was then mixed thoroughly with the Al powder at a pre-specified ratio. Four powder mixture samples, with the weight fractions of Al of 0.2, 0.4, 0.6 and 0.8, were prepared. The samples were compressed in cylindrical steel tubes under a pressure of 250 MPa using a hydraulic press. The steel tubes had an internal diameter of 21 mm and an external diameter of 25 mm. The resultant compacts had a diameter of 21 mm and a length of 30 mm. For each Al/NaCl compact, three thermal couples were embedded in radial distances of 0, 1.5 and 3 mm from the central position, as shown schematically in Fig. 1. Both ends of the compact were sealed by a thermal insulating material in order to minimize the axial heat flow. The compact, together with the steel tube, was then placed in an electrical furnace pre-heated to 650 °C. The variations of temperature with time at the three locations were recorded by a Picotech TC-08 data logger. The measurement terminated when the temperature of the central location reached 650 °C.

3. Computation of thermal diffusivity

An Al/NaCl compact is composed of Al, NaCl, air and Al_2O_3, which are greatly different in thermal properties. Because the Al and NaCl particles used for making the compact are relatively small and the compact is homogeneous from

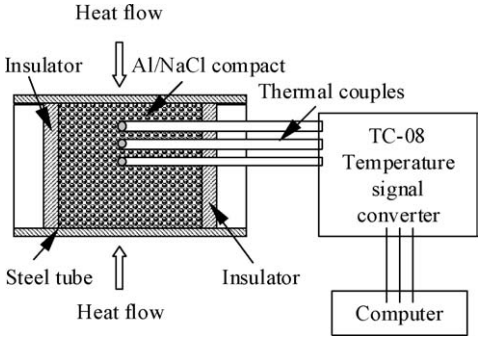

Fig. 1. Schematic of temperature measurement arrangement.

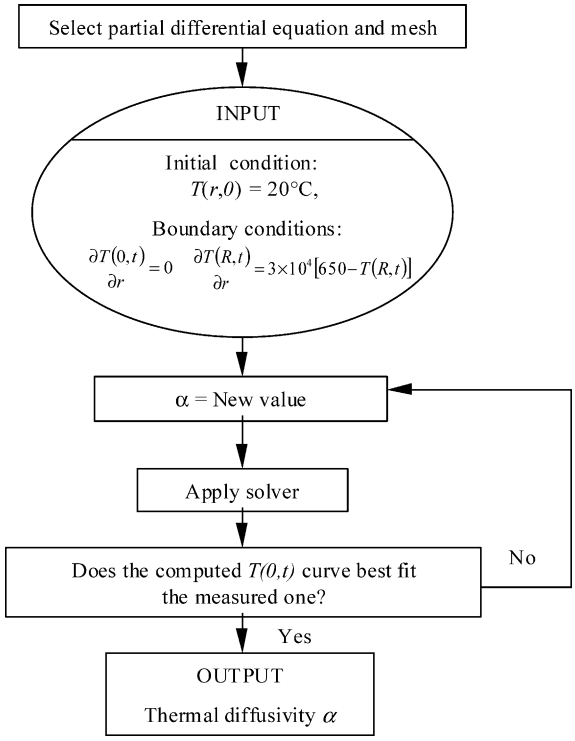

Fig. 2. Flow chart of numerical procedure for calculations of thermal diffusivities using Matlab 6.1.

a macroscopic point of view, however, the compact can be characterised by a single thermal diffusivity. Assuming that the thermal diffusivity is temperature-independent and there is no axial heat flow, the radial flow of heat in a cylindrical compact can be described by the following equation:

$$\frac{\partial T}{\partial t} = \alpha \left[\frac{1}{r}\frac{\partial T}{\partial r} + \frac{\partial^2 T}{\partial r^2} \right] \quad (1)$$

where T is temperature, r the radial distance, t the time and α is thermal diffusivity [15,16].

Matlab 6.1 was used to simulate the temperature variations with time in the Al/NaCl compact by solving Eq. (1). Fig. 2 shows the flow chart of the numerical procedure. The initial and boundary condition were assigned as close to the experimental conditions as possible. The compact was initially at room temperature before being heated, so the initial condition was assigned as $T(r,0) = 20\,^{\circ}\mathrm{C}$, where $T(r,t)$ designates the temperature at radial distance r at time t. At the center of the compact, there should be no net flow of heat. The boundary condition at $r = 0$ was, therefore, assigned as $\frac{\partial T(0,t)}{\partial r} = 0$. The boundary condition at the surface of the compact was established by estimating the heat flow across the interface between the compact and the steel tube. The heat flow rate is proportional to the local temperature gradient with the thermal conductivity as the proportionality coefficient. The local heat flow rates in the compact and the steel tube at the interface must be equal. With the temperature gradient across the thickness of the steel tube being treated as a constant, the temperature gradient at the surface of the compact can be expressed as a function of the surface temperature by:

$$\frac{\partial T(R,t)}{\partial t} = \frac{k_s}{k}\frac{T_0 - T(R,t)}{s} = h[T_0 - T(R,t)] \quad (2)$$

where R is the radius of the compact, k_s the thermal conductivity of the steel, k the thermal conductivity of the compact, s the thickness of the steel tube, T_0 the temperature of the furnace and h is a coefficient calculated from k_s, k and s. It should be noted that the thermal conductivity is related to the thermal diffusivity by $k = \alpha/\rho c$, where ρ is the density of the compact and c is the specific heat of the compact. ρc can be easily calculated from the densities and specific heats of Al and NaCl using the rule of mixture. Given α, h can be determined and Eq. (2) can serve as the surface boundary condition. Under the current conditions, the thermal conductivities of the compacts were found to be much lower than that of the steel and h was in the order of $10^4\ \mathrm{m}^{-1}$. The solution of Eq. (1) was largely determined by α and was insensitive to the changes in h. Even a deliberate large variation in h made no discernible difference to the simulated temperature profiles, except in the very beginning of the heating near the surface. In the present simulations, h was fixed at $3 \times 10^4\ \mathrm{m}^{-1}$ for simplification and T_0 at $650\,^{\circ}\mathrm{C}$.

The thermal diffusivity of each Al/NaCl compact was determined by comparing the simulated and measured temperature profiles at the centre of the compact. A series of α values were tried using the procedure in Fig. 2. For each α value, the history of the temperature distribution in the compact was generated by solving Eq. (1) with the above boundary conditions. The α value that generated the temperature versus time curve best fitting the measured curve was obtained as the thermal diffusivity of the compact. The simulated and measured temperature profiles at the other two locations, $r = 1.5$ and 3 mm, were also compared as an assurance measure.

4. Results and discussion

Fig. 3 shows the variations of the temperature at the center of the cylindrical Al/NaCl compacts with heating time obtained by the experimental measurements and computer simulations. The thermal diffusivities that generated the simulation curves were 2.63×10^{-7}, 3.03×10^{-7}, 3.45×10^{-7} and $3.70 \times 10^{-7}\ \mathrm{m}^2/\mathrm{s}$, corresponding to the Al weight fractions, w_{Al}, of 0.2, 0.4, 0.6 and 0.8. It can be seen that the simulated curves agreed well with the measured curves.

Fig. 4 shows the relationship between the thermal diffusivity and the Al weight fraction of the Al/NaCl compact. The thermal diffusivity of the compact increases approximately linearly with the weight fraction of Al in the compact. The thermal diffusivity of an Al/NaCl compact can, therefore, be predicted by the following empirical equation:

$$\alpha = (1.82 w_{\mathrm{Al}} + 2.30) \times 10^{-7} (\mathrm{m}^2/\mathrm{s}) \quad (3)$$

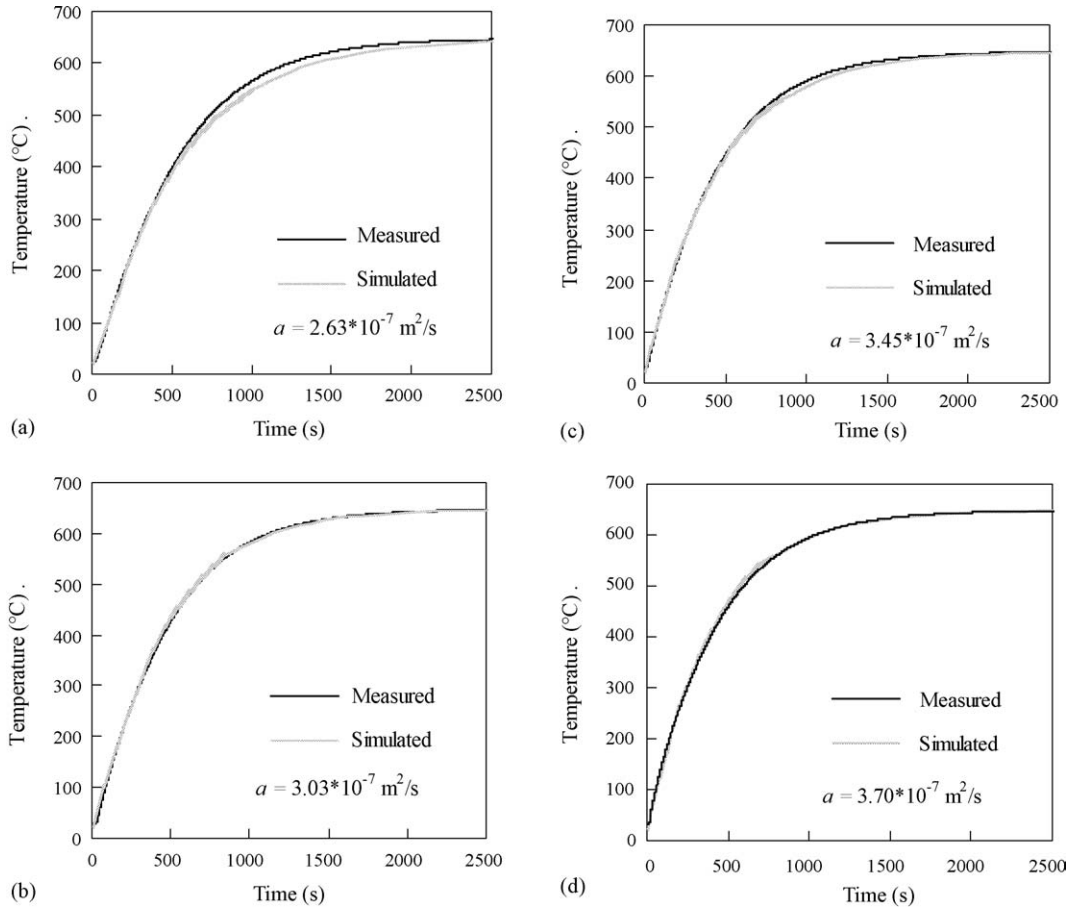

Fig. 3. Comparisons between measured and simulated temperature–time curves for the cylindrical Al/NaCl compacts with different Al weight fractions of (a) 0.2, (b) 0.4, (c) 0.6 and (d) 0.8.

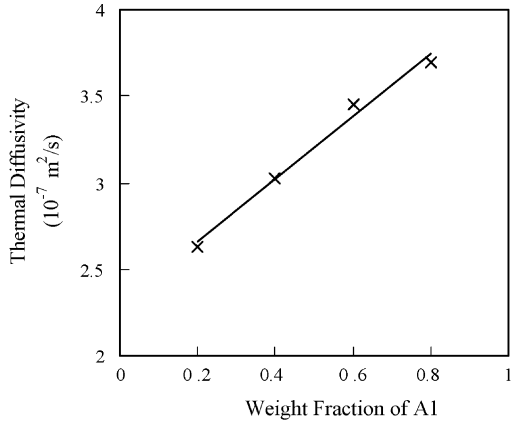

Fig. 4. Variation of thermal diffusivity of compact with Al weight fraction.

Table 1 shows the typical values of thermal conductivity, density, specific heat and thermal diffusivity of the constituents of an Al/NaCl compact, i.e., Al, NaCl, Al_2O_3 and air. The Al/NaCl compacts have lower thermal diffusivities than any of the constituents of the compacts. This was a surprise at first sight, but further analysis can show that the low thermal diffusivities are mainly due to the existence of air in the compacts, which has an extremely low thermal conductivity.

The thermal diffusivity of a compact consisting of several phases cannot be calculated directly from the thermal diffusivities of the constituent phases using the rule of mixture. It must be determined from the thermal conductivity, density and specific heat of the compact. By definition, $\alpha = k/\rho c$. The product of density and specific heat of the compact can be

Table 1
Thermal properties of Al, NaCl, Al_2O_3 and air at room temperature [17]

	Al	NaCl	Al_2O_3	Air
Conductivity (W/m K)	256	6.5	13	0.034
Density (g/m^3)	2.7×10^6	2.17×10^6	3.8×10^6	883
Specific heat (J/g K)	0.9	1.01	0.8	1
Diffusivity (m^2/s)	1.05×10^{-4}	2.97×10^{-6}	4.28×10^{-6}	3.85×10^{-5}

calculated using the rule of mixture:

$$\rho c = f_{\mathrm{Al}}\rho_{\mathrm{Al}}c_{\mathrm{Al}} + f_{\mathrm{NaCl}}\rho_{\mathrm{NaCl}}c_{\mathrm{NaCl}} + f_{\mathrm{Al_2O_3}}\rho_{\mathrm{Al_2O_3}}c_{\mathrm{Al_2O_3}} + f_{\mathrm{air}}\rho_{\mathrm{air}}c_{\mathrm{air}} \approx f_{\mathrm{Al}}\rho_{\mathrm{Al}}c_{\mathrm{Al}} + f_{\mathrm{NaCl}}\rho_{\mathrm{NaCl}}c_{\mathrm{NaCl}} \quad (4)$$

where f represents the volume fraction of a constituent in the compact, ρ density and c specific heat. The subscripts designate the respective constituents. The contributions from Al_2O_3 and air can be ignored because of the low volume fraction of Al_2O_3 and the low density of air.

The thermal conductivity of a compact consisting of several phases depends not only on the thermal conductivities of the constituents but also on the spatial distribution of the constituents. There is no simple analytical equation available for accurate predictions. However, the lower limit of the thermal conductivity of a compact can be calculated if the volume fractions of the constituents are known. Let us consider a uniformly mixed Al/NaCl/Al_2O_3/air compact of length l. Suppose that there is a steady longitudinal heat flow with a rate per unit area of J in the compact and a temperature difference of T is resulted. If a longitudinal fibre of infinitesimal cross-sectional area is taken from the compact, very few of the phase boundaries between the constituents are parallel to the fibre. The fibre can be seen as the four constituents, Al, NaCl, Al_2O_3 and air, in series, with their aggregate lengths of $f_{\mathrm{Al}}l$, $f_{\mathrm{NaCl}}l$, $f_{\mathrm{Al_2O_3}}l$ and $f_{\mathrm{air}}l$, respectively. The relationships between the heat flow rate and the temperature changes over the full length l and in the individual constituents in the fibre are described by the steady-state heat conduction equation:

$$J = -k\frac{\Delta T}{l} = -k_{\mathrm{Al}}\frac{\Delta T_{\mathrm{Al}}}{f_{\mathrm{Al}}l} = -k_{\mathrm{NaCl}}\frac{\Delta T_{\mathrm{NaCl}}}{f_{\mathrm{NaCl}}l} = -k_{\mathrm{Al_2O_3}}\frac{\Delta T_{\mathrm{Al_2O_3}}}{f_{\mathrm{Al_2O_3}}l} = -k_{\mathrm{air}}\frac{\Delta T_{\mathrm{air}}}{f_{\mathrm{air}}l} \quad (5)$$

where k represents thermal conductivity and ΔT temperature change. The subscripts designate the respective constituents. Because the overall temperature change in the fibre is the sum of the changes in the individual constituents, $\Delta T = \Delta T_{\mathrm{Al}} + \Delta T_{\mathrm{NaCl}} + \Delta T_{\mathrm{Al_2O_3}} + \Delta T_{\mathrm{air}}$ the thermal conductivity of the compact is therefore related to the thermal conductivities of the constituents by:

$$\frac{1}{k} = \frac{f_{\mathrm{Al}}}{k_{\mathrm{Al}}} + \frac{f_{\mathrm{NaCl}}}{k_{\mathrm{NaCl}}} + \frac{f_{\mathrm{Al_2O_3}}}{k_{\mathrm{Al_2O_3}}} + \frac{f_{\mathrm{air}}}{k_{\mathrm{air}}} \quad (6)$$

It can be seen that the thermal conductivity of the compact is predominantly determined by the constituent with the lowest thermal conductivity, which is air in this case. The contribution from Al_2O_3 can be ignored because of its low volume fraction. As an illustration,

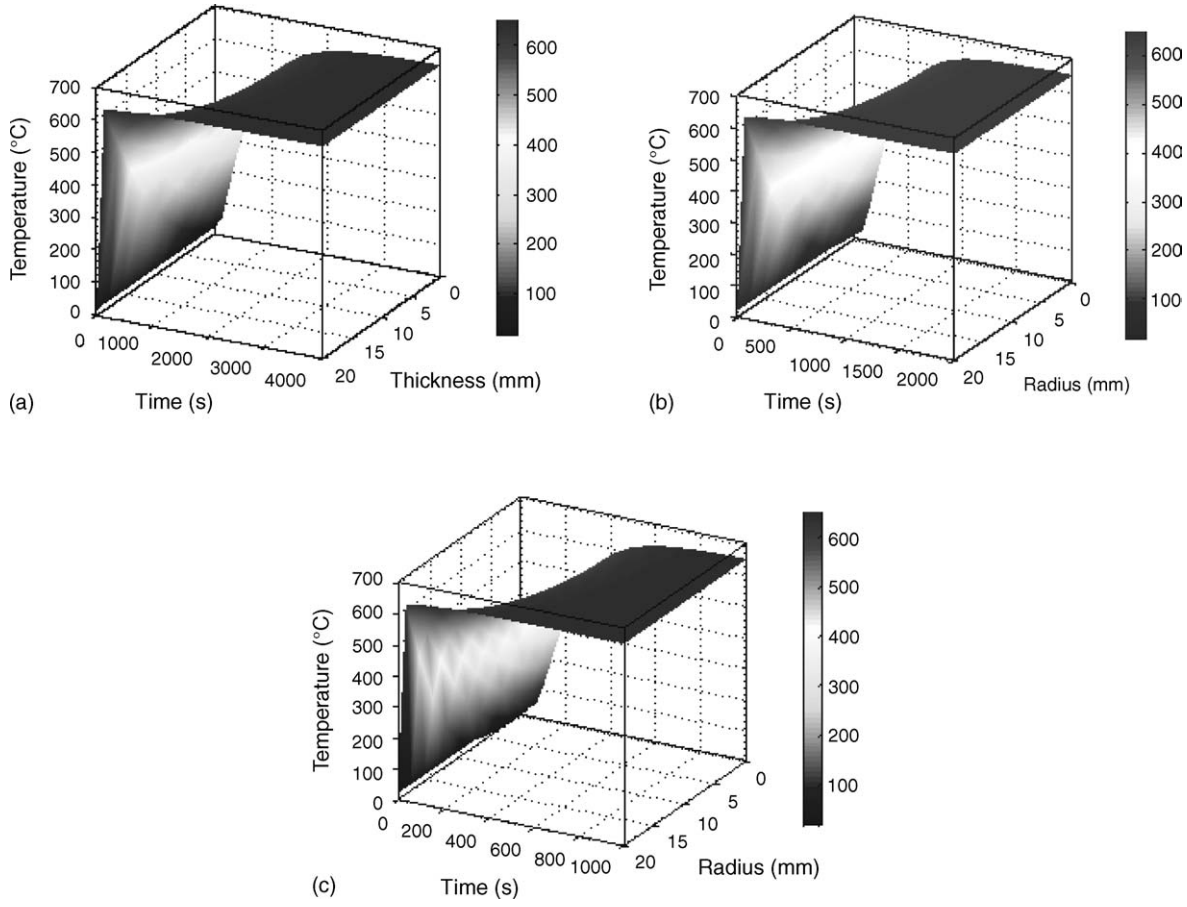

Fig. 5. Variations of temperature profile with time in Al/NaCl compacts with an Al weight fraction of 0.3 in the shape of (a) plate (b) cylinder and (c) sphere.

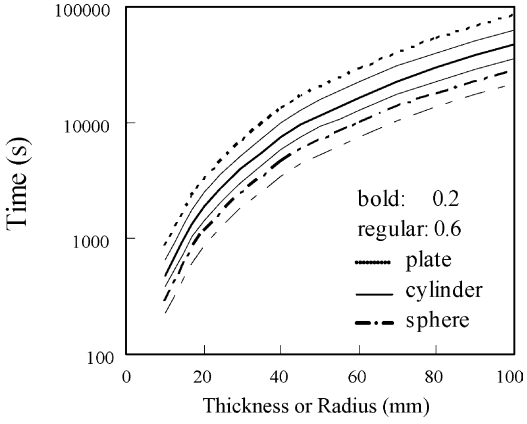

Fig. 6. Relationship between time needed for temperature homogenisation and sample size for plate, cylindrical and spherical Al/NaCl compacts with different Al weight fractions.

assuming that $f_{Al} = 0.47$, $f_{NaCl} = 0.47$, $f_{Al_2O_3} = 0.01$ and $f_{air} = 0.05$, $\rho c = 2.2 \times 10^6$ J/(m^3 K), $k = 0.65$ w/(m K) and $\alpha = k/\rho c = 3 \times 10^{-7}$ m^2/s.

The thermal diffusivities of the Al/NaCl compacts determined by the simulations are in the same order as that estimated by the above analytical analysis. In fact, the porosity of the Al/NaCl compacts compressed under a pressure of 200–300 MPa is normally between 5 and 10%, i.e., $f_{air} = 0.05$–0.1. The oxygen content of fine Al powders atomised in air is less than 1% [18]. Al_2O_3 in the Al/NaCl compacts is therefore normally less than 2%, i.e., $f_{Al_2O_3} < 0.2$. As an estimation, the thermal diffusivity of an Al/NaCl compact can be conveniently calculated from Equations (4) and (6).

From a practical point of view, the process parameter of interest is the heating time required for the successful sintering of an Al/NaCl compact. It is, therefore important to predict the time needed for the homogenization of temperature in a compact. Fig. 5(a–c) show the variations of the temperature profiles with time in the Al/NaCl compacts with a geometry of plate, cylinder and sphere, respectively, simulated using Matlab 6.1. In the simulations, the weight fraction of the Al/NaCl compacts was chosen to be 0.3 and the thermal diffusivity was obtained from Eq. (3) as 2.85×10^{-7} m^2/s. The half thickness or radius of the plate, cylinder or sphere was fixed at 20 mm. The heat conduction equation was modified for the cylinder and sphere. Fig. 6 shows the variations of homogenization time with size of plate, cylindrical and spherical compacts with typical Al weight fractions. The homogenization time was chosen as the time needed for the centre of the compact to reach 645 °C when the compact was placed into a furnace maintained at 650 °C. It is shown that for a fixed compact geometry and size, the homogenization time increases with the Al weight fraction decreased but the effect of Al weight fraction is not so pronounced. The homogenization time increases markedly with increasing plate thickness or cylinder radius. SDP is, therefore, not ideal for producing thick plates and rods because they require prolonged heating.

5. Conclusion

The thermal diffusivity of an Al/NaCl compact increases approximately linearly with the weight fraction of Al in the compact and can be approximated by the following empirical equation: $\alpha = (1.82 w_{Al} + 2.30) \times 10^{-7}$ m^2/s. The thermal diffusivity of the compact is much lower than those of both Al and NaCl, due to the existence of low-thermal-conductivity air in the compact. The homogenization time is mainly determined by the geometry and size of the compact. The effect of the Al weight fraction on the homogenization time is not significant in comparison.

References

[1] M.F. Ashby, et al., Metal Foams: A Design Guide, Butterworth Heinemann, 2000.
[2] A. Fuganti, L. Lorenzi, in: J. Banhart (Ed.), Metal Foams and Porous Metal Structures, Verlag MIT Publishing, Bremen, 1999, pp. 5–13.
[3] H. Seeliger, in: J. Banhart (Ed.), Metal Foams and Porous Metal Structures, Verlag MIT Publishing, Bremen, 1999, pp. 29–36.
[4] C. Haberling, et al., in: J. Banhart (Ed.), Metal Foams and Porous Metal Structures, Verlag MIT Publishing, Bremen, 1999, pp. 35–47.
[5] J.E. Siebels, in: J. Banhart (Ed.), Metal Foams and Porous Metal Structures, Verlag MIT Publishing, Bremen, 1999, pp. 13–23.
[6] R. Kretz, et al., in: J. Banhart (Ed.), Metal Foams and Porous Metal Structures, Verlag MIT Publishing, Bremen, 1999, pp. 23–29.
[7] C. Korner, R. Singer, Processing of metal foams—challenges and opportunities, Adv. Eng. Mater. 2 (2000) 159–165.
[8] T.J. Lu, A. Hess, M.F. Ashby, Sound absorption in metallic foams, J. Appl. Phys. 85 (1999) 7528–7539.
[9] T.J. Lu, H.A. Stone, M.F. Ashby, Heat transfer in open-cell metal foams, Acta Mater. 46 (1998) 3619–3635.
[10] L.J. Gibson, M.F. Ashby, Cellular Solids: Structure and Properties, second ed., Cambridge University Press, Cambridge, UK, 1997.
[11] G.J. Davies, S. Zhen, Metallic foams—their production, properties and applications, J. Mater. Sci. 18 (1983) 1899–1911.
[12] Y.Y. Zhao, D.X. Sun, A novel sintering-dissolution process for manufacturing Al foams, Scripta Mater. 44 (2001) 105–110.
[13] D.X. Sun, T. Fung, Y.Y. Zhao, in: J. Banhart (Ed.), Cellular Metals and Foaming Technology, Verlag MIT Publishing, Bremen, 2001, pp. 227–230.
[14] D.X. Sun, Y.Y. Zhao, Static and dynamic energy absorption of Al foams produced by the sintering and dissolution process, Metall. Mater. Trans. B 34 (2003) 69–74.
[15] S.J. Williams, Engineering Heat Transfer, PWS Engineering, Boston, 1986.
[16] H. Gröber, S. Erk, Fundamental of Heat Transfer, third ed., McGraw-Hill Book Company, INC, New York, 1961.
[17] D.R. Lide (editor in chief), CRC Handbook of Chemistry and Physics, CRC Press, Boca Raton, 2004.
[18] A. Unal et al., Production of aluminum and aluminum–alloy powder, in: ASM Handbook, vol. 7, ASM International, Materials Park, 1998, pp. 148–159.